

# Multiple laser pulses in conjunction with an optical clearing agent to improve the curative effect of cutaneous vascular lesions

Jun Ma<sup>1</sup> · Bin Chen<sup>1</sup> · Yue Zhang<sup>1</sup> · Dong Li<sup>1</sup> · Zhuang Lin Xing<sup>1</sup>

Received: 24 November 2016 / Accepted: 23 May 2017 / Published online: 3 June 2017  
© Springer-Verlag London 2017

**Abstract** Port-wine stains (PWSs) usually respond poorly to pulsed dye laser treatment because of the shallow penetration and light absorption of melanin in the epidermis. Multiple laser pulses (MLPs) Nd:YAG laser in conjunction with an optical clearing agent can help to reduce the total laser energy required for blood coagulation. The quantitative optical clearing effect (OCE) of glycerol was investigated by using a tissue-like phantom. Thereafter, an *in vitro* capillary tube experimental system and an *in vivo* hamster dorsal skin chamber experiment for the laser treatment of PWSs were established to visually obtain the quantitative relationship between the OCE and the blood coagulation properties under the irradiation of 1064 nm MLPs. Diffuse reflection coefficient decreases by 36.69% and transmission coefficient increases by 38.73% at 1064 nm, after applying 0.5 mL anhydrous glycerol for 10 min on the surface of the tissue-like phantom. The number of laser pulses required for blood coagulation decreases by 25% after the application of 0.5 mL anhydrous glycerol for 4 min, thrombosis appears after 10 min, and the 0.0854 clotting area completely blocks the capillary tubes in 6 pulses. For 10 min, the incident energy can be reduced by 35.09 and 29.82%. When the 0.3-mm vessel's buried depths are 1 and 0.5 mm, the pulse number can be reduced from 11 to 8 and from 6 to 4, respectively. Adding anhydrous glycerol directly on the hamster dorsal skin is an effective way to reduce the number of laser pulses from 4~5 to 2~3 for similar capillary tube diameter. Therefore, the MLPs of 1064 nm Nd:YAG demonstrates a substantial curative effect for large

capillary tubes. In conjunction with glycerol, this approach may treat deeply buried cutaneous capillary tubes and prevent the unwanted thermal damage of normal dermal tissue.

**Keywords** Multiple laser pulses · Optical clearing effect · Nd:YAG laser · Port-wine stain · Tissue-like phantom · Blood coagulation

## Introduction

Port-wine stain (PWS) birthmarks are a congenital microvascular malformation of the skin that occurs in 0.3 to 0.5% of newborns [1]. PWSs are usually located near the eyes, lips, or joints and can psychologically distress a patient [2]. Based on selective photothermolysis theory [3], pulsed dye laser (PDL) at wavelengths of 585 and 595 nm has become the gold standard therapy to thermally damage PWS vessels by the photo-coagulation of hemoglobin. However, a considerable number of patients do not achieve complete lesion removal with PDL treatment. Incomplete PWS blanching can be ascribed to shallow penetration because of the short wavelength and high absorption of epidermal melanin; this phenomenon both reduces the light deposition in large and deeply buried PWS vessels [4].

Recently, near-infrared Nd:YAG laser at the 1064-nm wavelength has attracted the attention of researchers because of its deep penetration and low melanin absorption [5]. Promising results have been obtained, particularly in purple, hypertrophic, and nodular PWS lesions. Yang et al. [6] stated that a 1064-nm Nd:YAG laser used at the minimum purpura dose (MPD) was effective for treating intractable PWSs. Li et al. [7] compared the thermal response of blood vessels under the irradiation of 595 nm pulse dye laser and 1064 nm Nd:YAG laser. They found that hemorrhage is the main

✉ Bin Chen  
chenbin@mail.xjtu.edu.cn

<sup>1</sup> State Key Laboratory of Multiphase Flow in Power Engineering, Xi'an Jiaotong University, Xi'an, Shaanxi 710049, China

thermal response of blood vessels under 595 nm laser; therefore, the induced purpura is serious. In comparison, the main thermal response of the Nd:YAG laser is the disappearance of blood vessels owing to uniform heating. Nevertheless, high energy is required for sufficient photocoagulation by Nd:YAG laser because of low hemoglobin absorption. However, this condition can cause surrounding tissue thermal damage because of the relatively high water absorption. Yang et al. [6] indicated that a single-pulse Nd:YAG laser can cause significant scarring when using energy exceeding 1.2 times the MPD. Thereafter, safe treatment is difficult for anatomically heterogeneous vascular lesions, such as PWSs. Jia et al. [8] suggested that the MLPs approach is a promising alternative therapy for inducing blood vessel photocoagulation at lower laser energy per pulse than single-laser pulse (SLP). Fournier et al. [9] successfully used MLPs to treat leg telangiectasia. Wu et al. [10] used MLPs Nd:YAG to irradiate vessels in the dorsal skin chamber and found that this approach causes vessel expansion, blood coagulation, and vasoconstriction. From a thermophysical point of view, the principle of MLPs is that the delivery of subsequent pulses before blood vessels cool to the baseline temperature can increase the temperature of blood vessels to a higher degree than SLP [11]. From a biological point of view, MLPs induce the summation of irreversible thermal injury from a series of low-peak temperature heating cycles. The temperature of the vessel irradiated by multiple laser increases with the number of laser pulses when the time interval between two laser pulses is short [12]. Jia et al. [13] reported that HbO<sub>2</sub> in blood vessels was converted into MetHb after irradiated by Nd:YAG laser, which could enhance the absorption coefficient of blood. Hence, the laser treatment of PWSs may be improved by using an MLPs Nd:YAG laser. However, cumulative pulses increased the extent of tissue injury, including both desired vascular changes and unwanted effects, such as extravasation [14]. Therefore, a new strategy is required to reduce the incident energy to spare the surrounding tissue.

Early studies by Tuchin et al. [15–19] demonstrated that hyperosmotic agents can significantly increase the optical transparency of skin and other turbid tissues, thus potentially reducing laser energy. Currently used optical clearing agent (OCA) includes glycerol [20], dimethyl sulfoxide [21], and propanediol [22] with refractive index of 1.47, 1.479, and 1.43, respectively. Considering that the optical clearing effect (OCE) increases with the refractive index, propanediol is a poor option. Dimethyl sulfoxide possesses a high refractive index but could stimulate the skin and respiratory tract. People prefer to use glycerol as the OCA because it possesses a high refractive index with no side effects. Jiang et al. [23] studied OCE under a 1000–1700-nm wavelength and found that OCE increases with the glycerol concentration in tissue-like phantoms [24]. Vargas et al. [25] injected anhydrous glycerol into hamster skin and indicated that the light transmittance increased by 50% after 20 min. Furthermore,

Vargas et al. [26] reported that a hyperosmotic agent applied to skin prior to 532 nm laser irradiation could decrease the radiant exposures required for photocoagulation. The addition of glycerol to dorsal blood vessels resulted in altered blood flow which is stopped by using the Doppler optical coherence tomography [27]. Complete flow cessation of blood in vessels before laser irradiation can significantly decrease the energy required to permanently destroy a blood vessel [28]. The stratum corneum can block the entry of foreign matter into the skin tissue. In clinical application, the stratum corneum structure can be disrupted by polishing with sandpaper [29] or applying Azone [30].

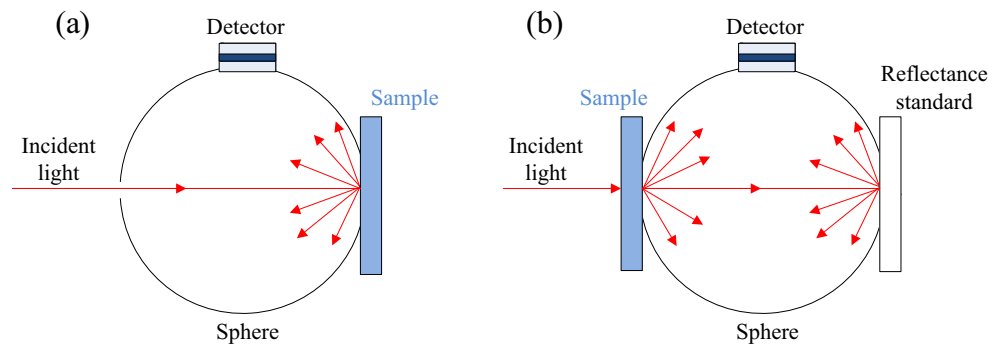
In summary, available results have demonstrated that the addition of glycerol to the skin and blood vessels can increase light penetration and laser deposition to the target vessel, thus reducing the incident laser energy and preventing the thermal damage of normal skin tissue. However, the quantitative study of the optical clearing induced by a hyperosmotic agent is still lacking. Furthermore, new strategies regarding the combination of OCA with MLPs Nd:YAG laser in PWS treatment have not been reported. In this work, to investigate the effect of glycerin dosage, concentration, and penetration time on OCE, we introduced a tissue-like phantom containing blood vessels with stable optical properties to eliminate the influence of skin physiological structure and individual differences. Afterwards, an *in vivo* animal experiment was also conducted on blood vessels in hamster dorsal skin to explore a new treatment strategy by combining OCA with MLPs Nd:YAG laser and optimizing the OCA and laser parameters in the treatment of cutaneous vascular lesions.

## Effect of glycerol on the OCE of tissue-like phantom

### Theoretical basis of the optical clearing technique

Laser light propagation in the skin is a combination of scattering and absorption. Scattering greatly affects the depth of light penetration, which occurs mainly in the dermis. Therefore, the epidermis is not taken into consideration when studying the effect of glycerol on reducing the scattering coefficient of the skin. From a physiological structure point of view, the dermis tissue is composed of different cell clusters embedded in a web that is immersed in liquid matrix. Collagen and elastic fibers accounted for approximately 70% of the weight of the dermis. From the optics perspective, the different scales of fiber and cell constitute a similar scattering turbid medium of ingredients. The refractive index of different ingredients in skin tissue varies. The refractive index of elastic fibers and collagen fibers is approximately 1.47 [15], the refractive index of nucleus and organelles is between 1.38 and 1.41 [31], and the refractive index of the background

**Fig. 1** Single integrating sphere system. **a** Diffuse reflection measurement. **b** Transmittance measurement



water-based matrix is approximately 1.36 [17]. When light propagates through the skin tissue, strong scattering effect exists because of refractive index mismatch, i.e., the difference between the elastic fibers and water-based matrix [15]. The following formula can be used to measure the matching degree of the refractive index between the scattering component  $n_s$  and water-based matrix  $n_0$ :

$$m = n_s / n_0, \quad (1)$$

The scattering properties of skin tissue can be measured by the decreased scattering characteristics [30]:

$$\mu'_s = 3.28\pi a^2 \rho_s \left(2\pi a / \lambda\right)^{0.37} (m-1)^{2.09}, \quad (2)$$

where  $a$  is the average radius of the scattering particles,  $\rho_s$  is the number of scattering particles per unit volume, and  $\lambda$  is the wavelength of incident light.

From Eq. (1), the reduced scattering coefficient becomes smaller when  $m$  is closer to 1. The basic principle of OCE is that the high permeability and high index of the refraction agent can replace the moisture in dermal tissue, and the resulting dehydration can effectively decrease the value of  $n_0$ . By contrast, the permeation of the high refractive index agent to the dermal tissue will match the refractive index of the scattering component and water-based matrix, thus aiding in the improvement of light penetration depth in skin tissue.

## Materials and methods

In this study, a tissue-like phantom was employed to investigate the OCE of glycerol. Compared with real

skin, the tissue-like phantom possesses stable optical properties and can eliminate the influence of complicated tissue structures. To prepare the tissue-like phantom, Indian ink (1.2 vol%, Beijing Solarbio Science and Technology Co. Ltd., China), Intralipid (2 vol%, Huarui Pharmaceutical Co. Ltd., China), and agar powder (1.5%, Sigma Co. Ltd., USA) were selected as absorber, scatterer, and basic material, respectively. The highly purified agar powder was dissolved in 50 mL distilled water at 70 °C. The mixture was stirred, heated to 95 °C, and placed in a 70 °C water bath. Considering that the agar solution alone possesses negligible absorption and extremely low turbidity, appropriate amounts of Indian ink as absorber and Intralipid as scatterer should be added. The optimal temperature for mixing these substances with the agar solution is 70 °C. At this temperature, the solution should be stirred continuously while being cooled to 50 °C. At 50 °C, the solution must be poured into a mold composed of a glass plate with a chamber (30 mm × 25 mm × 1 mm) to be assembled to the desired size. Finally, the solution was pressed with a covering glass. After 2 min, the phantom can be taken from the mold and then measured.

Given its high permeability and high refractive index, we chose glycerol (Shanghai Biological Engineering Technology Co. Ltd.) as OCA to study the OCE by the tissue-like phantom. A glycerol-distilled water solution was prepared at different concentrations (60, 80, and 100% glycerol) for the experiment. Prior to the experiment, glycerol was directly applied to the surface of the tissue-like phantom. A UV/VIS/NIR spectrophotometer (U4100, Hitachi Company, Japan) with a single integrating sphere

**Table 1** OCE of skin tissue-simulating phantoms with different concentrations of glycerol (penetration time is 10 min)

Glycerol volume	Glycerol concentration (%)	Diffuse reflection (%)	$(R_0 - R) / R_0$ (%)	Transmission (%)	$(T - T_0) / T_0$ (%)
0.5 ml	60	20.06	25.43	40.19	22.30
	80	19.11	28.96	47.34	33.81
	100	17.03	36.69	49.10	38.73

**Table 2** OCE of skin tissue-simulating phantoms with different penetration times of glycerol

Glycerol volume	Glycerol concentration	Time	Diffuse reflection (%)	$(R_0 - R)/R_0$ (%)	Transmission (%)	$(T - T_0)/T_0$ (%)
0.5 ml	100%	2	23.53	12.52	40.10	15.89
		4	21.23	21.08	42.09	18.97
		6	19.68	26.81	45.20	27.75
		8	18.96	29.51	46.43	31.23
		10	17.03	36.69	49.10	38.73
		12	17.05	36.62	49.49	39.89
		14	17.19	36.31	49.47	39.85

was employed to measure the diffuse reflection spectrum and transmission spectrum of the tissue-like phantoms at 1064 nm. As shown in Fig. 1a, the standard piece is placed at the back of a hole to scan a baseline, and the sample was placed at the same location to measure the diffuse reflection. In comparison, we placed the sample in front of the hole after scanning the baseline to measure transmittance (Fig. 1b). Each experiment was repeated 5 times in our manuscript.

### OCE of tissue-like phantom at 1064 nm

After five identical phantom samples were prepared, the diffuse reflection spectrum and transmission spectrum were measured one after another by a UV/VIS/NIR spectrophotometer to test the optical stability of the phantoms at 1064 nm. The average diffuse reflection spectrum and transmission spectrum of the tissue-like phantoms are 26.9 and 35.4%, respectively. The standard deviations of the diffuse reflection coefficient and transmission coefficient of the five different tissue-like phantoms are 0.78, 0.9, 0.44, 0.53, and 0.38% and 1.24, 1.43, 1.46, 1.34, and 1.21%, separately. The results demonstrate the excellent stability of the tissue-like phantom, which is suitable for studying the OCE of glycerol.

The principle of OCE is as follows: the concentration of glycerol is high on the surface of tissue-like phantoms, thus leading to the influx of glycerol molecules with a high refractive index of 1.47 into the tissue under the action of osmotic pressure. Water molecules with a low refractive index of 1.33 will be squeezed out of the tissue-like phantoms by glycerol

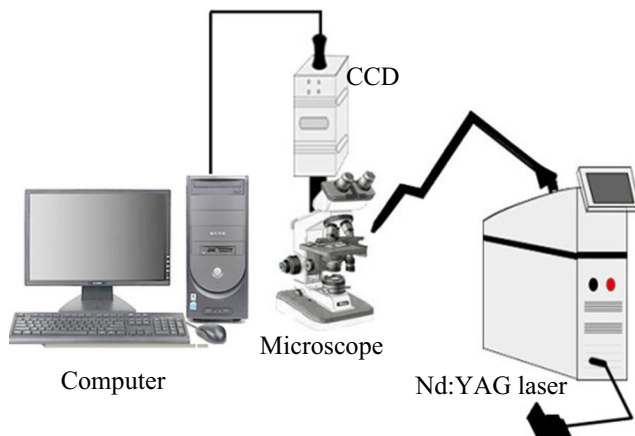
molecules. The glycerol molecules with a high refractive index replaced water with a low refractive index, which increase the refractive index of the basic material and decrease the relative refractive index of the scattering particles and decrease the scattering coefficient. The increase in refractive index of the interstitial fluid decreases the relative refractive index of the scattering particles and decreases the scattering coefficient. Fick's second law can be used to describe the diffusion of glycerol molecules in the tissue-like phantom. A higher glycerol concentration leads to a better diffusion effect and better OCE. The replacement of distilled water in the tissue-like phantom by the high refractive index of glycerol, as well as the dehydration of bio-tissue induced by OCA, leads to refractive index matching in turbid tissue, thus decreasing light scattering. In this section, we introduce tissue-like phantoms to study the influence of glycerin dosage, concentration, and penetration time on OCE at 1064 nm.

Table 1 illustrates the variation in diffuse reflection and transmittance of the phantom with different concentrations of glycerol after 10 min of penetration by 0.5 mL glycerol. A higher glycerol concentration can result in a smaller diffuse reflection coefficient and higher transmittance coefficient. The decrease in diffuse reflection coefficient compared with that of the original phantom is 25.43, 28.96, and 36.69% when the concentrations of glycerol are 60, 80, and 100%, respectively; furthermore, the increase in transmittance coefficient compared with that of the original phantom is 22.30, 33.81, and 38.73% when the concentrations of glycerol are 60, 80, and 100%. Therefore, anhydrous glycerin yielded the best optical effect.

**Table 3** OCE of skin tissue-simulating phantoms with different volumes of glycerol (penetration time is 10 min)

Glycerol concentration	Glycerol volume (mL)	Diffuse reflection (%)	$(R_0 - R)/R_0$ (%)	Transmission (%)	$(T - T_0)/T_0$ (%)
100%	0.25	20.12	25.20	43.88	24.03
	0.5	17.03	36.69	49.10	38.73
	0.75	16.99	36.84	48.99	38.47



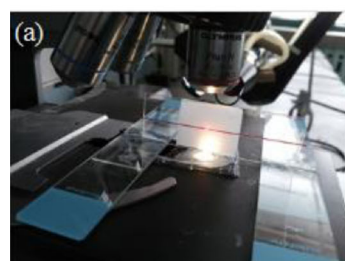


**Fig. 2** Experimental system for laser treatment of PWS

Table 2 shows the diffuse reflection coefficient and transmittance coefficient of the phantom as a function of time after the application of 0.5 mL anhydrous glycerol. The diffuse reflection coefficient of the phantom decreased with the penetration time after the application of glycerol, whereas the transmittance coefficient increased with penetration time. After 2 min of anhydrous glycerol penetration, the OCE is markedly enhanced. The decrease in the diffuse reflection coefficient and the increase in transmittance coefficient compared with those of the original phantom are 36.69 and 38.73%, respectively, after 10 min of penetration by anhydrous glycerol. After 12 and 14 min, no apparent change on OCE was observed compared with that after 10 min. Therefore, the optimal penetration time of glycerol is 10 min.

Table 3 presents the variation in diffuse reflection and transmittance of the phantom with different volumes of anhydrous glycerol after 10 min of penetration. Applying 0.5 mL anhydrous glycerol to the surface of the phantom results in a superior OCE compared with that of 0.25 mL, whereas 0.75 mL anhydrous glycerol yielded similar effects with 0.5 mL. The diffuse reflection at 0.25, 0.5, and 0.75 mL decreased by 25.20, 36.69, and 36.84% compared with the control group, respectively; by contrast, transmittance at 0.25, 0.5, and 0.75 mL increased by 24.03, 38.73, and 38.47%, respectively.

**Fig. 3** Schematic of the in vitro and in vivo model. **a** Tissue-simulating phantom. **b** Dorsal skin chamber



## Effect of the OCA on the laser treatment of PWSs

The above results demonstrate that smearing glycerol on the surface of the tissue-like phantom can markedly improve tissue optical transmittance. To obtain the quantitative relationship between OCE and the blood coagulation properties by 1064 nm MLPs Nd:YAG laser, a set of in vitro (Fig. 3a) and in vivo (Fig. 3b) experiments were conducted to mimic the laser treatment of PWSs. For the in vitro experiment, a glass capillary tube (inner diameters of 0.3 and 0.2 mm) filled with fresh human venous blood sample from a healthy male donor was fixed on the bottom of the tissue-like phantom to simulate the abnormal capillary tube, as shown in Fig. 3a. A Nd:YAG laser (Fig. 2) (Won-Cosjet TR, Won Technology Co. Ltd., Korea) will pass through the tissue-like phantom and irradiate the glass capillary tube, thus effectively simulating the laser treatment of PWSs. We use ethylenediaminetetraacetic acid anticoagulant to prevent coagulation of blood. The laser hand piece was positioned such that the central part of the blood column in each capillary was irradiated in the exact same geometry.

The addition of glycerol to dorsal capillary tubes could alter blood flow [17]. The influence of flow cessation of blood on the number of laser pulses of 1064 nm Nd:YAG laser is unclear. So a hamster dorsal skin flap window (Fig. 3b) was needed to study the effect of glycerol directly on the capillary tubes. In this in vivo experiment, dorsal capillary tubes of female Sprague-Dawley (SD) hamster with 100~120 g body weight were used to prepare the dorsal skin flap window, which were provided by the Animal Center of Medical School in Xi'an Jiaotong University. Before the implantation of chamber plates, a hamster was under deep anesthesia with celiac injection of chloral hydrate anesthesia, with the dorsal area of each hamster shaved and epilated to remove hair roots. Then, a twofold skin at the shaved spot was lifted, and one side was marked with a 1-cm diameter circle for the position of the observation window. Next, to expose vessels and clearly observe the microcirculation, the entire epidermis, dermis, and subcutaneous connective tissue of the marked circle were carefully removed. Finally, the DSC model was accomplished by placing two chamber plates at each side of the twofold skin

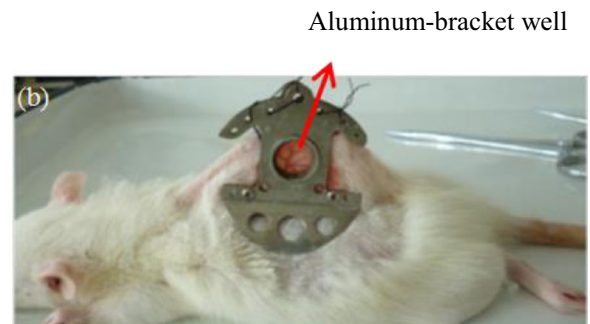


**Table 4** Laser parameters

Parameter	Wavelength (nm)	Pulse width (ms)	Spot size (mm)	Energy density ( $\text{J}/\text{cm}^2$ )	Pulse number, $n_p$	Frequency (Hz)
Value	1064	0.3	2	30–57	1–15	10

with covering glass to the exposed skin surface, and bolts were used to hold the chamber plates together. This allowed direct observation of capillary tubes of the subdermal skin. The subcutaneous side of the window contained a circular aluminum bracket (as shown in Fig. 3b) well approximately 2 mm deep and 1 cm in diameter fixed directly on the exposed subcutaneous skin. Anhydrous glycerol at a concentration of 100% was applied to the subdermal side of the skin for 20 min, filling the volume of the well against the skin. The glycerol was continually replaced whenever the level went down, because there was leakage of the fluid from the well through the edge. Any remaining glycerol was removed at the end of 20 min.

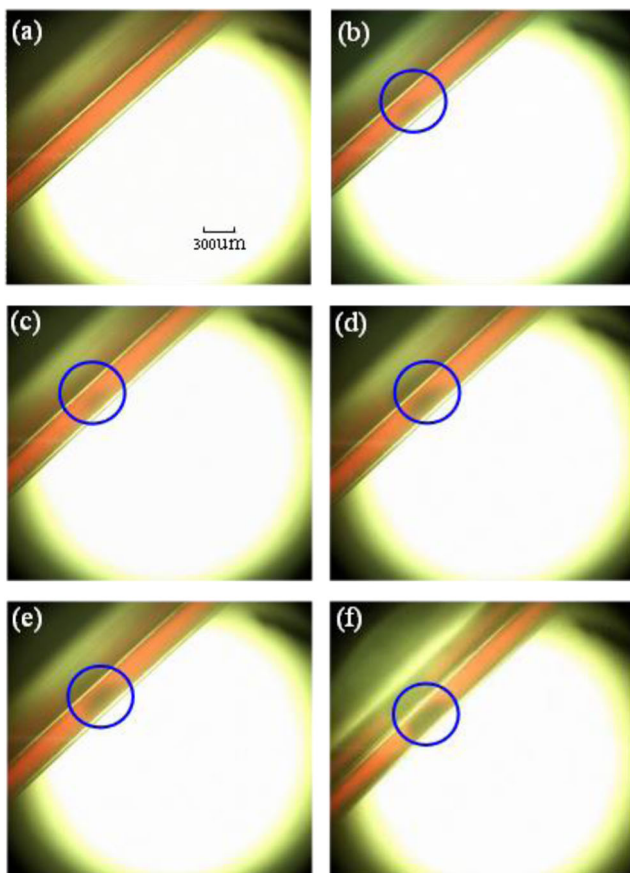


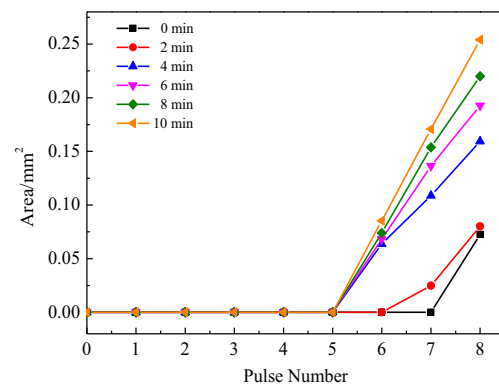
**Fig. 4** Effect of glycerol on the number of laser pulses required for blood coagulation. No glycerol, **a**  $n_p = 7$ , no thrombus appeared; **b**  $n_p = 8$ , thrombus appeared. With glycerol for 4 min, **c**  $n_p = 6$ , thrombus appeared but cannot block the blood vessel; **d**  $n_p = 7$ , thrombus blocked the blood vessel. With glycerol for 10 min, **e**  $n_p = 6$ , thrombus blocked the blood vessel; **f**  $n_p = 7$ , thrombus blocked the blood vessel

A high-speed camera (Redlake, HG-100K, USA) with a resolution of 1504 pixels  $\times$  1128 pixels and frame rate of 25–2000 fps, together with a microscope imaging system (U-TVO.63XC, Olympus, Japan), was employed to record blood coagulation under different numbers of laser pulses. The Nd:YAG laser parameters used in this experiment are listed in Table 4.

### Relationship between the penetration time of glycerol and blood coagulation

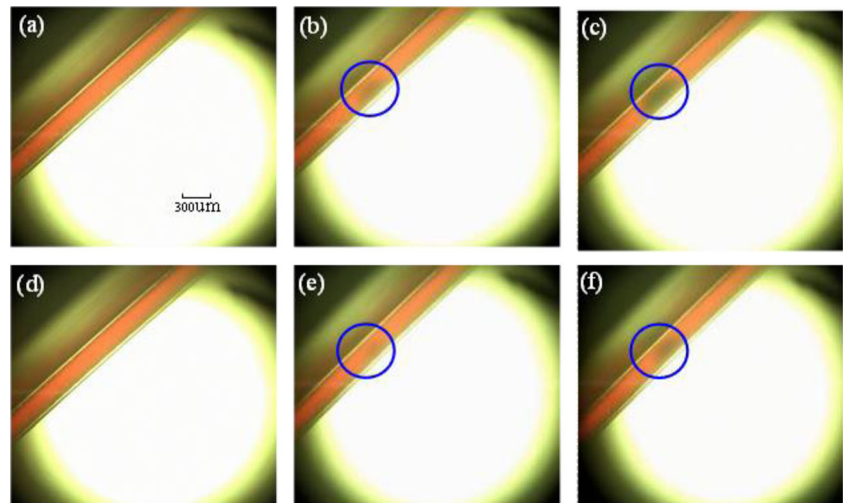
The anhydrous glycerol of the same volume of 0.5 mL was smeared on the surface of tissue-like phantom (30 mm  $\times$  25 mm  $\times$  1 mm) with different penetration times (0, 2, 4, 6, 8, 10, 12, and 14 min). Thereafter, we studied the quantitative relationship between glycerol penetration time and the number of laser pulses required for blood coagulation under the effect of multipulse Nd:YAG laser. The image analysis software Image-Pro Plus 6.0 was used to calculate the blood coagulation area. We used a 53-J/cm<sup>2</sup> radiant exposure, and the pulse frequency was 10 Hz.

Figure 4 exemplifies the influence of glycerol penetration time on the number of laser pulses required for blood clotting (dark area). When no glycerol was applied on the surface of the tissue-like phantom, there is no thrombus in capillary tubes after undergoing 7 laser pulses, and the thrombus appeared immediately after 8 pulses. Therefore, the number of laser pulses required for blood coagulation is 8. After the application of anhydrous glycerol on the surface of tissue-like phantom for 4 min, the number of laser pulses required for blood coagulation decreased to



**Fig. 5** Effect of glycerol on blood coagulation area and the number of laser pulses

**Fig. 6** Effect of glycerol on the laser incident energy density required for coagulating blood buried at the depth of 1 mm. **a–c** No glycerol, 57 J/cm<sup>2</sup> ( $n_p = 6, 7,$  and 8, from *left to right*). **d–f** With glycerol for 10 min 37 J/cm<sup>2</sup> ( $n_p = 6, 7,$  and 8, from *left to right*) ( $i_d = 0.3$  mm)



6, but the thrombus was not evident. Afterwards, the thrombus blocks the capillary tubes after the 7th pulse. For 10 min, the pulse number did not continue to reduce; however, coagulation can block the capillary tubes after a 6-laser pulse. So the 6-laser pulse is an optimal choice. The thrombus that completely blocks the vessel is the prerequisite for a thread-like appearance, which is the desirable clinical end point. Figure 5 plots the effect of glycerol infiltration time on the blood clot area and the number of laser pulses. Each group is repeated 5 times and every data point in Fig. 5 is the average coagulation area of the 5 capillary tubes. With the increase in glycerol penetration time, the blood coagulation area gradually increased in the 6th pulse. However, no thrombus formation was observed when the penetration time was 0 or 2 min. Figure 4f shows that thrombosis can completely block capillary tubes in 6 pulses after 10 min of applying 0.5 mL anhydrous glycerol on the surface of the tissue-simulating phantom. The blood

coagulation area is 0.0854 mm<sup>2</sup> measured by the Image-Pro Plus (Fig. 5). For the best clinical treatment result, the formation of blood clots should only block the capillary tube. Therefore, the best treatment strategy is for thrombosis to block capillary tubes in 6 pulses after 10 min of applying 0.5 mL anhydrous glycerol.

#### Effect of glycerol on incident energy density

The effect of glycerol on incident energy density for blood coagulation was explored with an incident energy density of 57–37 J/cm<sup>2</sup> and frequency of 10 Hz. For the control group, no glycerol was applied on the tissue-simulating phantom, which was irradiated with energy of 57 J/cm<sup>2</sup> to record the number of laser pulses required for blood coagulation. The number of laser pulses that thrombus appeared was regarded as the criteria for evaluating the effect of glycerol on blood coagulation for two reasons: (1) the appearance of the

**Fig. 7** Effect of glycerol on the laser incident energy density required for coagulating blood buried at the depth of 0.5 mm. **a–c** No glycerol, 57 J/cm<sup>2</sup> ( $n_p = 2, 3,$  and 4, from *left to right*). **d–f** With glycerol for 10 min, 40 J/cm<sup>2</sup> ( $n_p = 2, 3,$  and 4, from *left to right*) ( $i_d = 0.3$  mm)

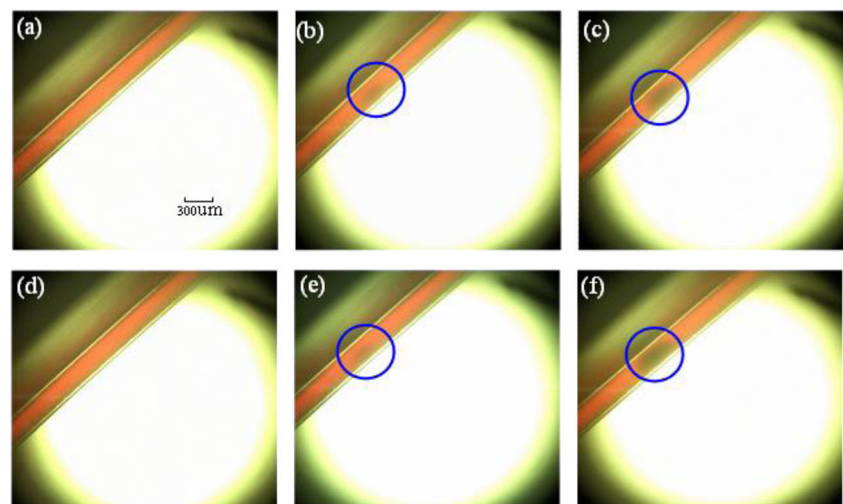
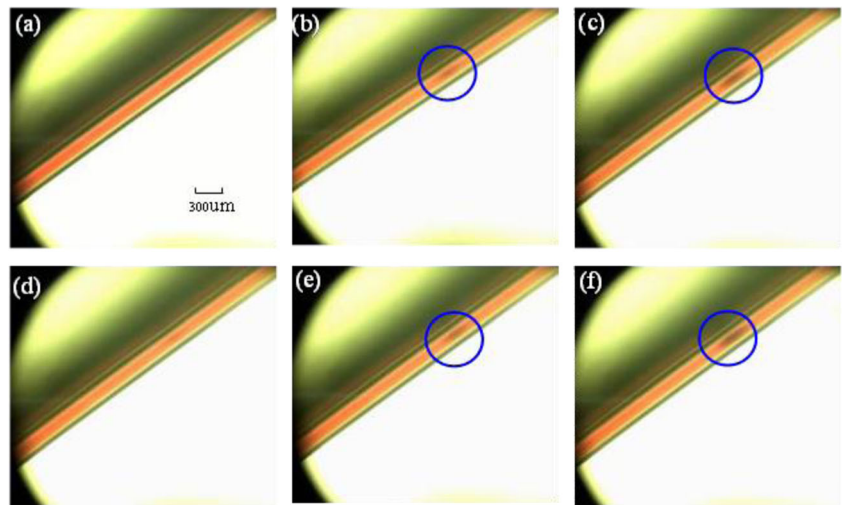




**Fig. 8** Effect of glycerol on the laser incident energy density required for coagulating blood buried in the tissue-simulating phantom at the depth of 1 mm and with an inner diameter of 0.2 mm. **a–c** No glycerol, 57 J/cm<sup>2</sup> ( $n_p = 10, 11,$  and 12, from *left to right*). **d–f** With glycerol for 10 min, 47 J/cm<sup>2</sup> ( $n_p = 10, 11,$  and 12, from *left to right*)



thrombus means the desirable thermal response of the capillary tube, which has been proved in our previous DSC animal experiment; and (2) the lower number of pulses was chosen because it is the least energy dose for a desirable thermal response.

For the experimental group, 0.5 mL anhydrous glycerol was smeared on the surface of the tissue-simulating phantom (length 30 mm, width 25 mm, thickness 1 and 0.5 mm, respectively) for 10 min. The laser pulse or incident energy density was gradually reduced by 2 J/cm<sup>2</sup> until the thrombus appeared at the recorded number of laser pulses with the control group. Therefore, the number of laser pulses required for blood coagulation in the control group and experimental group was consistent. It is the thrombus that appears and blocks the capillary tube that determines the laser parameters. Then, we can explore the effect of OCA on laser incident energy density.

Figures 6 and 7 present the effect of glycerol on the laser incident energy density required for coagulating the capillary

tube buried in the tissue-simulating phantom with a diameter of 0.3 mm at depths of 1 and 0.5 mm. When the buried depth was 1 mm (Fig. 6), the incident energy density required for blood coagulation at 7 laser pulses was 57 J/cm<sup>2</sup> for the control group (Fig. 6a–c). However, for the experimental group (Fig. 6d–f), the incident energy density required for blood coagulation decreased to 37 J/cm<sup>2</sup> at the same pulse number. When capillary tubes were buried at the depth of 0.5 mm (Fig. 7), the incident energy density required for blood coagulating at 3 laser pulses was 57 J/cm<sup>2</sup> for the control group (Fig. 7a–c), whereas the incident energy density decreased to 40 J/cm<sup>2</sup> after the application of glycerol for 10 min (Fig. 7d–f).

Figures 8 and 9 show the effect of glycerol on the laser incident energy density required for coagulating the capillary tube buried in the tissue-simulating phantom with a diameter of 0.2 mm at depths of 1 and 0.5 mm. With the buried depth of 1 mm (Fig. 8), the incident energy density required for blood coagulation at 11 laser pulses was 57 J/cm<sup>2</sup> for the control group (Fig. 8a–c). For the experimental group, the incident

**Fig. 9** Effect of glycerol on the laser incident energy density required for coagulating blood buried in the tissue-simulating phantom at 0.5 mm and with an inner diameter of 0.2 mm. **a–c** No glycerol, 57 J/cm<sup>2</sup> ( $n_p = 5, 6,$  and 7, from *left to right*). **d–f** With glycerol for 10 min, 53 J/cm<sup>2</sup> ( $n_p = 5, 6,$  and 7, from *left to right*)

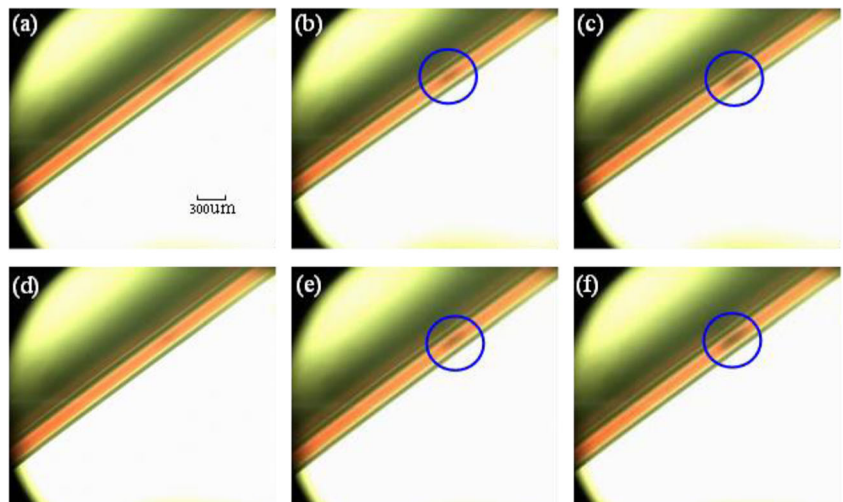




**Table 5** Summary of effect of glycerol on incident energy density

ID (mm)	Depth (mm)	$n_p$	Control group $E_0$ ( $J/cm^2$ )	Experimental group $E_1$ ( $J/cm^2$ )	$(E_0 - E_1) \times 100/E_0$ (%)
0.3	0.5	3	57	40	29.82
	1.0	7	57	37	35.09
0.2	0.5	6	57	53	7.02
	1.0	11	57	47	17.54

energy density decreased to  $47 J/cm^2$  (Fig. 8d–f). When the capillary tube was buried to a depth of 0.5 mm (Fig. 9), the incident energy density required for blood coagulation at 3 laser pulses is  $57 J/cm^2$  for the control group (Fig. 9a–c). The incident energy density reduced to  $53 J/cm^2$  after the application of glycerol for 10 min (Fig. 9d–f). The result is summarized in Table 5. Glycerol has an obvious effect on reducing the incident energy density. When the capillary tubes are buried deeper, the effect of glycerol became more obvious. After the application of glycerol for 10 min, the incident energy can be reduced by 35.09 and 29.82% compared with the control group when the vessel with 0.3 mm inner diameter was buried at depths of 1 and 0.5 mm.

#### Effect of glycerol on the total number of pulses

To explore the effect of glycerol on the total number of pulses required for blood coagulation, we irradiated vessels with different buried depths and diameters. For the experimental group, 0.5 mL anhydrous glycerol was smeared on the surface of the tissue-simulating phantom (length 30 mm, width 25 mm, thickness 1 and 0.5 mm) for 10 min. For the control group, no glycerol was applied on the tissue-simulating phantom. Two capillary glass tubes with inner diameters of 0.2 and 0.3 mm were selected.

The results with the incident laser energy density of  $57 J/cm^2$  and pulse repetition rate of 10 Hz are shown in Figs. 10,

11, 12, and 13. Figures 10 and 11 illustrate the effect of glycerol on the total number of laser pulses required for coagulating the capillary tube with a diameter of 0.3 mm buried in the tissue-simulating phantom with depths of 1 and 0.5 mm, respectively. In the control group, the pulse numbers required for coagulating the blood were 7 and 3 for depths of 1 (Fig. 10a–c) and 0.5 mm (Fig. 11a–c), respectively. In the experimental group, the pulse number decreased to 4 (Fig. 10e) and 2 (Fig. 11e). Figures 12 and 13 show the effect of glycerol on the total number of laser pulses when the vessel diameter was 0.2 mm. As seen from the results, the pulse number decreased from 11 (Fig. 12b) and 6 (Fig. 13b) to 8 (Fig. 12e) and 4 (Fig. 13e) for different buried depths of 1 and 0.5 mm, respectively.

Figures 10 and 13 confirm that glycerol exhibits considerable potential in reducing the total number of pulse required for blood coagulation when the frequency is 10 Hz. More experiments were conducted at different frequencies (5–10 Hz) for  $R_E$  per pulse of  $57 J/cm^2$ . Figure 14 shows the results for capillary tubes at different depths. We may conclude that glycerol is effective for reducing the total number of pulses required for blood coagulation when the frequency was changed from 5 to 10 Hz. Moreover, the pulse number did not increase with the decrease in frequency within a certain range. However, beyond this range, the number of laser pulses required to coagulate blood increases with the reduction in frequency. For different burial depths and vessel diameters,

**Fig. 10** Effect of glycerol on the total number of laser pulses required for coagulating blood buried in the tissue-simulating phantom at a depth of 1 mm and with an inner diameter of 0.3 mm. Incident energy density,  $57 J/cm^2$ . **a–c** No glycerol ( $n_p = 6, 7,$  and  $8,$  from left to right). **d–f** With glycerol for 10 min ( $n_p = 3, 4,$  and  $5,$  from left to right)

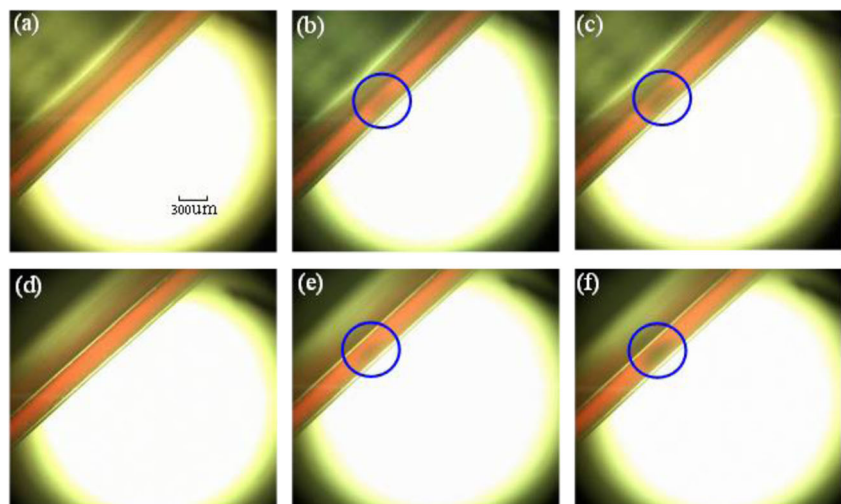
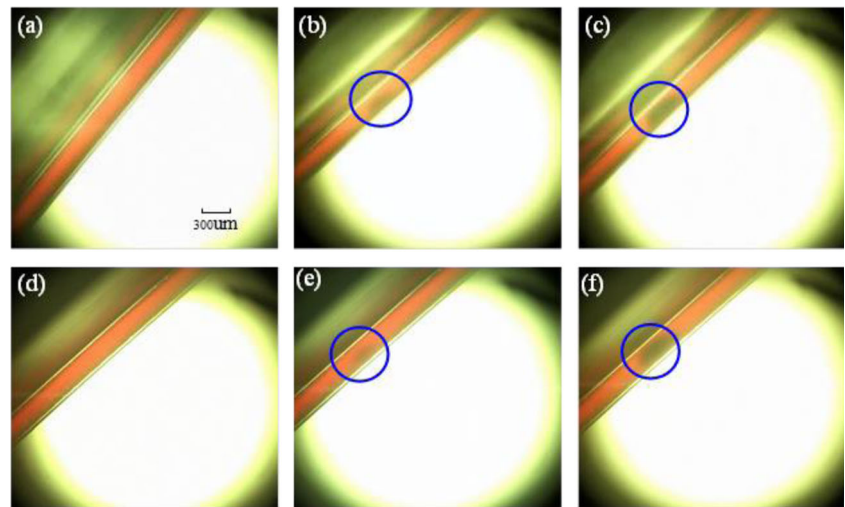


**Fig. 11** Effect of glycerol on the total number of laser pulses required for coagulating blood buried in the tissue-simulating phantom 0.5 mm, as the inner diameter is 0.3 mm, incident energy density is  $57 \text{ J/cm}^2$ . **a–c** No glycerol ( $n_p = 2, 3,$  and  $4$  from left to right). **d–f** With glycerol for 10 min ( $n_p = 1, 2,$  and  $3,$  from left to right)



an optimal frequency exists. For a fixed number of laser pulses, a low laser frequency should be selected in the treatment of vascular diseases, as shown in Fig. 14. The effective treatment of 1064 nm laser involves the complete photocoagulation of vessels. In the case of total incident energy unchanging, a certain frequency range may allow the capillary tubes to be completely blocked. Then, we should select a low frequency to be able to block capillary tubes exactly. As listed in Table 6, the effect of glycerol for deeply buried capillary tubes is evident. Blood clotting is significantly better for large capillary tubes than small vessels because of the greater reduction in pulse number.

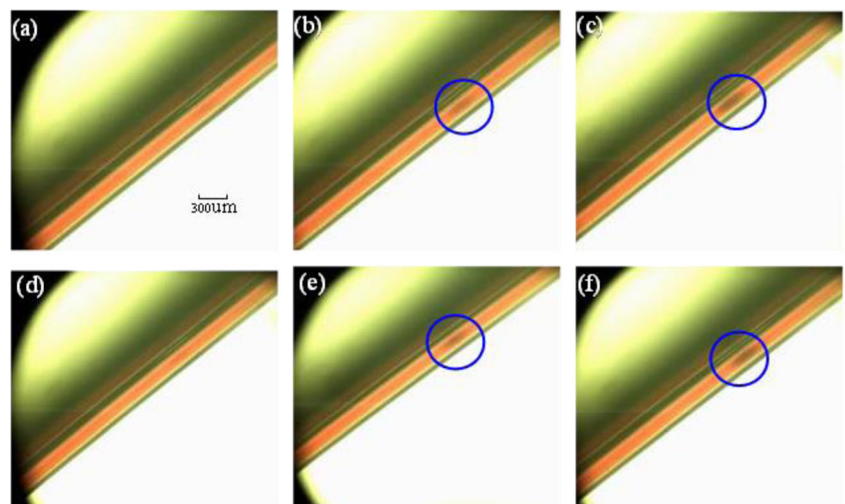
### Effect of glycerol on the capillary tubes

A total of 24 vessels were directly irradiated by 1064 nm Nd:YAG laser. The incident energy was  $37 \text{ J/cm}^2$ . We analyzed the response of the capillary tube to laser irradiation and

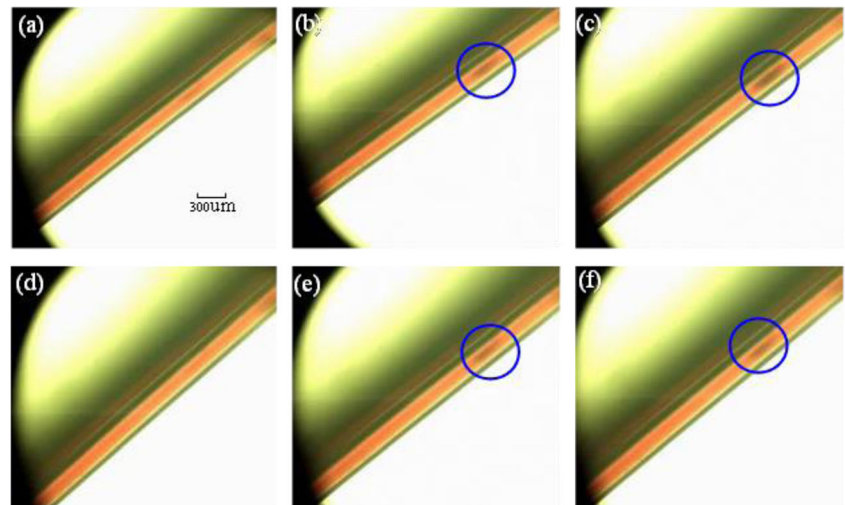
recorded the number of laser pulses required for blood coagulation.

Figure 15a, b shows the skin before and after a 20-min application of glycerol in the subdermal side of the hamster dorsal window. We can see that the application of anhydrous glycerol to the subdermal tissue leads to changes in skin optics. The capillary tube in Fig. 15b is clearer than that in Fig. 15a. We can even see the fluff hamster dorsal skin to be clear, as shown in the circle in Fig. 15. After applying glycerol on capillary tubes, an obvious shrinkage of small arteries and slight dilation of the venule can always be observed, which are pointed out by one-way and two-way arrows, respectively. The reason can be explained by the possible inflammatory response induced by the tissue in response to osmotic equilibrium deviations [32, 33]. In an acute inflammatory response, the diameter of the capillary tube increased, especially for the venule because its wall is on average thinner than the corresponding arteriole. Lowell found that the inner capillary tubes were correlated with blood flow rates. Decrease blood flow

**Fig. 12** Effect of glycerol on total number of laser pulses required for coagulating the blood buried at the depth of 1 mm, as the inner diameter is 0.2 mm (incident energy density is  $57 \text{ J/cm}^2$ ). **a–c** No glycerol ( $n_p = 10, 11,$  and  $12,$  from left to right). **d–f** With glycerol for 10 min ( $n_p = 7, 8,$  and  $9,$  from left to right)



**Fig. 13** Effect of glycerol on the total number of laser pulses required for coagulating blood buried at the depth of 0.5 mm, as the inner diameter is 0.2 mm (incident energy density is  $57 \text{ J/cm}^2$ ). **a–c** No glycerol ( $n_p = 5, 6,$  and  $7$ , from *left to right*). **d–f** With glycerol for 10 min ( $n_p = 3, 4,$  and  $5$ , from *left to right*)



velocity will cause decreased shear stress and constriction of the capillary tube [34]. The addition of glycerol to dorsal capillary tubes resulted in complete flow cessation. The shear stress of the arterial capillary tubes is reduced larger than that of the venule, as arterial blood flows faster. Therefore, the constriction rate is bigger in the arterial capillary tubes. In the artery, dilation rate is less than the contraction. In the venule, however, dilation rate is slightly bigger than the contraction. Thus, obvious shrinkage of small arteries and slight dilation of the venule can always be observed.

For the hamster dorsal window without pretreatment by glycerol, we counted the total number of laser pulses required for blood coagulation of 12 capillary tubes with different diameters ranging from 100 to 130  $\mu\text{m}$ . The site of laser irradiation is marked by yellow circles. The result in Fig. 16 confirms that the number of laser pulses required for blood photocoagulation (dark in the images) is 4–5. More experiments should be conducted to determine the effect of glycerol on the number of laser pulses required for blood coagulation. After

applying anhydrous glycerol for about 20 min, 12 capillary tubes ranging 100–130  $\mu\text{m}$  were irradiated by Nd:YAG laser 1064 nm MLPs in the control group. The site of laser irradiation is marked by blue circles. As shown in Fig. 17, the blood completely coagulated after 2–3 laser pulses. We may conclude that the infiltration of glycerol to the capillary tubes is effective on reducing the number of laser pulses required for blood coagulation.

## Discussion

In the section “Effect of glycerol on the OCE of tissue-like phantom,” we demonstrated that the optical properties of skin tissue, namely, the diffuse reflection coefficient and transmission coefficient, would be altered by the application of glycerol on the surface of the tissue-simulating phantom. The increase in transmission coefficient and reduction of diffuse reflection coefficient proved that the penetration depth of light

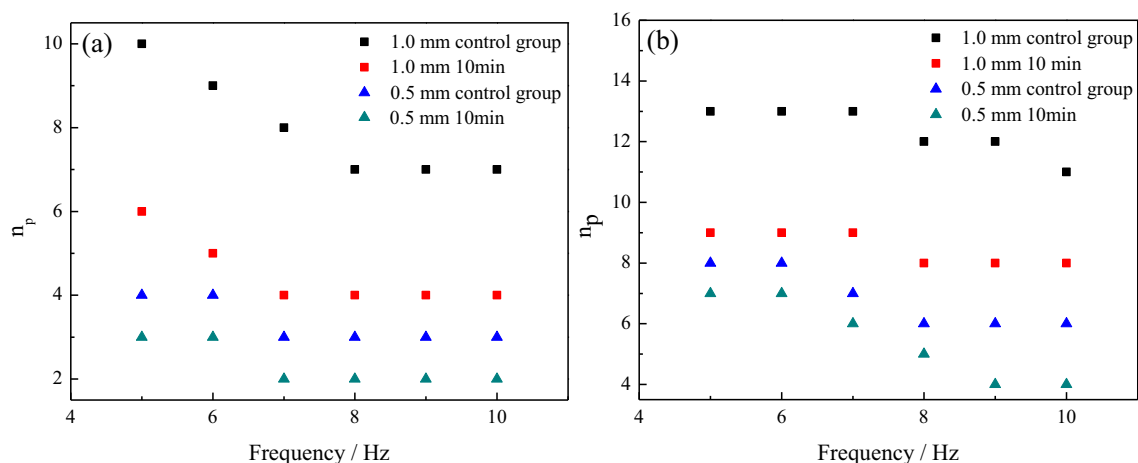


**Fig. 14** Effect of glycerol on the total number of laser pulses under different frequencies: with inner diameters of **a** 0.0 and **b** 0.2 mm (blood vessels buried at the depths of 1 and 0.5 mm, respectively)



**Table 6** Summary of effect of glycerol on total number of pulses

ID (mm)	Depth (mm)	$E_0$ (J/cm <sup>2</sup> )	Control group $n_p$	Experimental group $n_p$	$(E_0 - E_1) \times 100/E_0$ (%)
0.3	0.5	57	3	2	33.33
	1.0		7	4	42.85
0.2	0.5		6	4	33.33
	1.0		11	8	27.27

into skin can be improved evidently. The penetration depth will increase with glycerol infiltration time and concentration. The number of laser pulses required for blood coagulation decreased by 25% after the application of 0.5 mL anhydrous glycerol for 4 min. After 10 min, the number of laser pulses did not continue to decrease, but the area of blood coagulation increased by 34.1% compared with that for 4 min. Infiltration time appears to considerably influence blood coagulation as the energy reaching the vessels increases with time. However, an upper bound of time was observed. Once this limit was exceeded, the effect of glycerin will remain unchanged. The result of this experiment provides a reference for the optimum time for using glycerol.

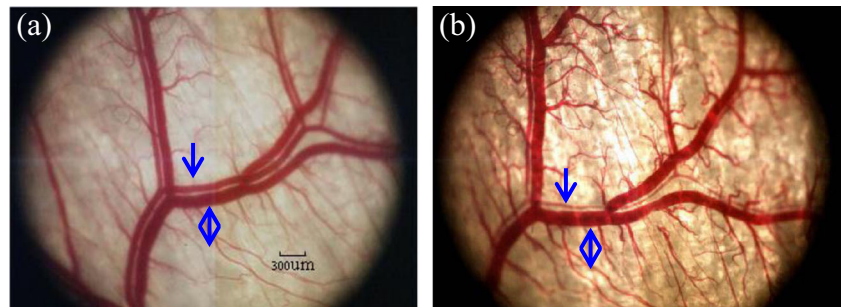
In terms of laser incident energy density, applying glycerin on the surface of tissue-simulating phantom for 10 min can effectively reduce the laser incident energy density needed for blood clotting at the same number of laser pulse compared with the control group. The inner diameter of the vessels and the depth of the vessels considerably have an influence on laser incident energy. When the capillary tubes are more deeply buried, more laser energy is lost in transmission owing to scattering and absorption. The smaller capillary tubes will be cooled rapidly during the interpulse interval; therefore, higher incident energy density may be required to clot the blood, which possibly causes thermal damage to normal skin tissue owing to the high absorption of water under long wavelength. The required incident energy density for blood clotting is not only dependent on the depth and diameter of the vessels but also on the optical properties of the skin. The addition of glycerol to the skin surface can significantly improve the optical properties, reduce the reflection coefficient, and increase the transmission coefficient. Thus, laser energy reaching the target capillary tubes may increase, leading to the reduction of

incident energy density. Considering there is almost no absorption by glycerol at this wavelength, glycerin infiltration and replacement of water in skin tissue can further reduce the thermal damage of dermal tissue. Besides, lower laser energy density can reduce pain during treatment.

For a fixed vessel depth, the pulse number needed to clot a capillary tube with 0.3 mm diameter is less than a capillary tube with 0.2 mm diameter. This finding may be attributed to the 1064-nm multipulse laser, which exhibits deep penetration depth in the skin tissue and blood. Furthermore, the large diameter of capillary tubes under this wavelength can be uniformly heated. When the diameter of capillary tubes is large, the absorption coefficient of hemoglobin and water in the blood under a 1064-nm wavelength is higher. When the diameter of the capillary tubes is larger, the thermal relaxation time is longer, and the heat dissipation rate is lower. Therefore, the accumulation of heat in large vessels under a laser pulse is higher than small capillary tubes. Hence, small capillary tubes need a large number of laser pulses to induce blood clotting. However, cumulative pulses can increase the extent of tissue injury, including both desired vascular changes and unwanted effects, such as extravasation. The addition of glycerin can significantly reduce the required number of laser pulses in blood clotting, possibly reducing thermal damage to dermal tissue. Moreover, the water absorption ability is stronger than that of glycerin under 1064 nm wavelength; therefore, the high permeability of glycerol replaces the moisture in the dermal and further reduces thermal damage to dermal tissue.

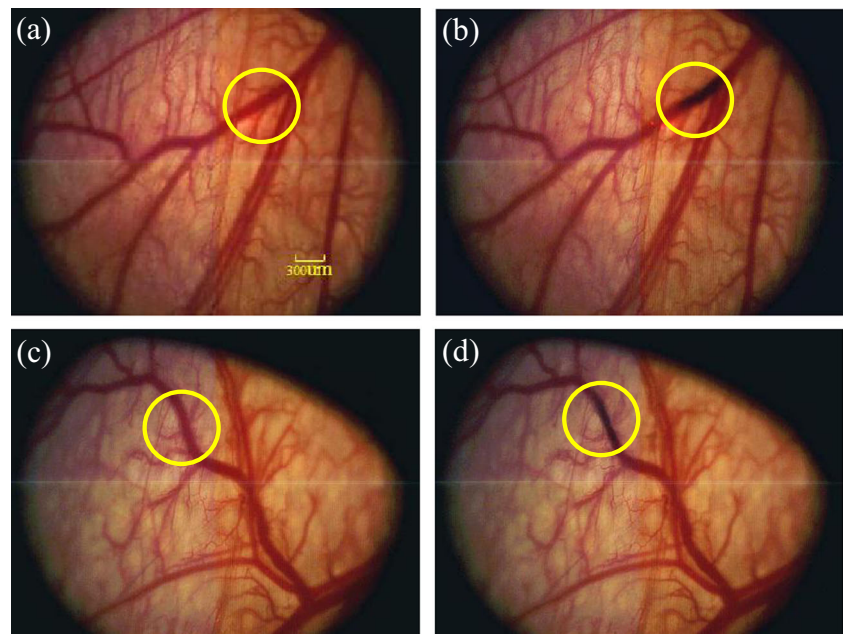
Frequency exerts a significant impact on the number of laser pulses required for blood clotting. A lower frequency requires more pulses for blood clotting. Increasing the frequency can reduce the pulse number. From a thermophysical point of view, the main criterion for determining frequency is

**Fig. 15** Subcutaneous side of the hamster dorsal skin flap window preparation. **a** Native skin. **b** Same window preparation 20 min following pretreatment with glycerol, *one-way arrows* pointing to arteries and the *two-way arrows* pointing to venule





**Fig. 16** Without pretreatment with glycerol, subcutaneous side of the hamster dorsal skin flap window preparation. Blood vessel before (a, c) and after the 4th (b) pulse and 5th (d) pulse, with energy density of  $37 \text{ J/cm}^2$  and pulse frequency of 10 Hz



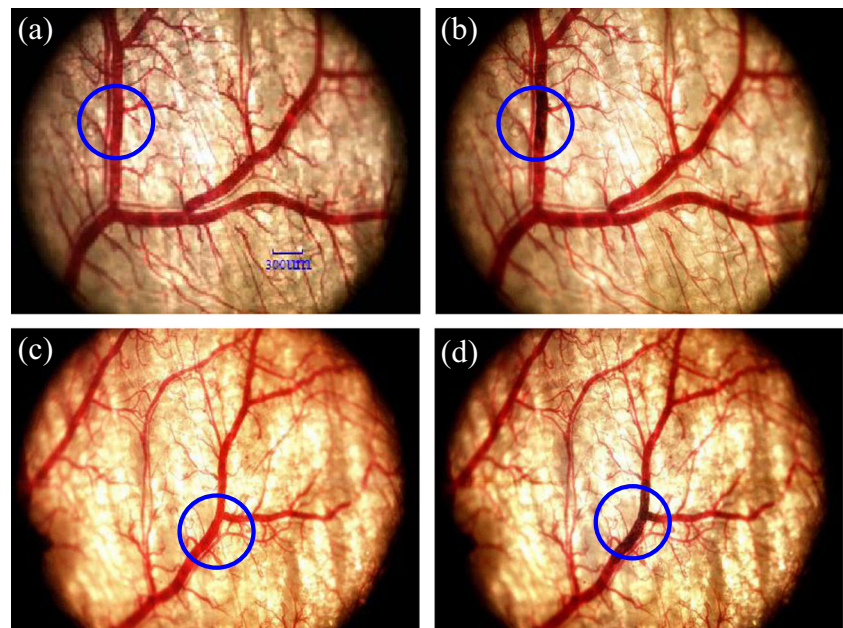
that a significant portion of heat generated by successive laser pulses accumulates in the targeted PWS capillary tubes. Therefore, the core temperature of the intravascular capillary tube increases substantially with each subsequent laser pulse, i.e., the blood temperature reaches the highest level after a pulse, and then heat is transferred to the surrounding tissue before the next pulse arrives.

Figure 14 provides the relationship between laser frequency and the diameter of capillary tubes. For a larger diameter, we can select low frequency. The addition of glycerin cannot always reduce the frequency but can significantly reduce the required number of laser pulses in blood clotting. High

frequency may cause thermal damage by accumulating energy, whereas low frequency could lead to failure in treatment. This experiment provides an approach to optimize laser frequency when using glycerol.

Adding glycerol directly on the subcutaneous side of the hamster dorsal could make the skin become more optically translucent due to reduction in light scattering in the dermis and blood. Previous studies have proved that complete flow cessation of capillary tubes before irradiation significantly reduces the energy required to permanently destroy the vessel [17]. However, when glycerol permeated into the blood, the scattering coefficient of the blood could be reduced.

**Fig. 17** Pretreatment with glycerol for 20 min, subcutaneous side of the hamster dorsal skin flap window preparation. Blood vessel before (a, c) and after the 2nd (b) pulse and 3rd (d) pulse, with energy density of  $37 \text{ J/cm}^2$  and pulse frequency of 10 Hz



Therefore, a decrease in light scattering may in fact increase the radiant exposures required for vessel stasis, because some photons contributing to photocoagulation may include those scattered into capillary tubes from the periphery [35]. The results of Figs. 16 and 17 indicated that applying anhydrous glycerol directly to the subcutaneous side of the hamster dorsal skin was an effective way to reduce the number of laser pulses from 4~5 to 2~3 at the same capillary tube diameter. It is evident that flow cessation of capillary tubes before irradiation plays a more important role in decreasing the number of laser pulses.

## Conclusion

In this paper, we introduced tissue-like phantoms with stable optical properties to quantitatively investigate the OCE by glycerol of different volumes, concentrations, and penetration times in the visible to near-infrared wavelengths. Results show that the best OCE can be obtained by smearing 0.5 mL anhydrous glycerol on the surface of tissue-like phantoms for 10 min. The diffuse reflection coefficient is reduced by 36.69%, and the transmission coefficient increases by 38.73% under the 1064-nm Nd:YAG laser.

Afterwards, an in vitro experimental system for the laser treatment of PWSs was set up to obtain a quantitative relationship between OCE and blood coagulation properties under the irradiation of 1064 nm MLPs Nd:YAG laser. Our conclusions are as follows:

1. After the application of 0.5 mL anhydrous glycerol for 10 min on the surface of the tissue-simulating phantom, the number of laser pulses required for blood coagulation decreases by 25%, and the blood clotting area is 0.0854 mm<sup>2</sup>, only blocking capillary tubes with 0.3 mm diameter cross section.
2. The curative effect for large diameter capillary tubes buried in the phantom by MLPs Nd:YAG laser is superior to small vessels. When using glycerol simultaneously, the 1064-nm laser can treat deeply buried capillary tubes and reduce possible thermal damage to normal dermal tissue.
3. Glycerol is effective for reducing the pulse number required for laser coagulation of capillary tubes when the frequency was changed from 5 to 10 Hz. The number of laser pulses required for blood coagulation separately decreased by 40 and 42.9% at 5 and 10 Hz after the application of 0.5 mL anhydrous glycerol for 10 min on phantom.
4. Applying anhydrous glycerol directly to the subcutaneous side of the hamster dorsal skin is an effective way to reduce the number of laser pulses from 4~5 to 2~3 at the same capillary tube diameter.

DSC experimental results show that combining MLPs Nd:YAG laser can help to reduce the total laser energy required for blood coagulation, especially for larger diameter and deeply buried capillary tubes. Therefore, they may also help to improve the laser treatment of cutaneous vascular lesions, and in vivo research will be conducted in the near future.

## Compliance with ethical standards

**Conflict of interest** The authors declare that they have no conflict of interest.

**Funding** This work was jointly supported by the National Natural Science Foundation of China (51336006) and the Fundamental Research Funds for the Central University.

**Ethical approval** All procedures performed in studies involving human participants were in accordance with the ethical standards of the institutional and/or national research committee and with the 1964 Helsinki declaration and its later amendments or comparable ethical standards.

**Informed consent** Informed consent was obtained from all individual participants included in the study.

## References

1. Schneider BV, Mitsuhashi Y, Schnyder UW (1988) Ultrastructural observations in port wine stains. *Arch Dermatol Res* 280(6):338–345
2. Barsky SH, Rosen S, Geer DE, Noe JM (1980) The nature and evolution of port wine stains: a computer-assisted study. *Invest Dermatol* 74(3):154–157
3. Anderson RR, Parrish JA (1983) Selective photothermolysis: precise microsurgery by selective absorption of pulsed radiation. *Science* 220(4596):524–527
4. Chen JK, Ghasri P, Aguilar G et al (2012) An overview of clinical and experimental treatment modalities for port wine stains. *J Am Acad Dermatol* 67(2):289–304
5. Liu S, Yang C, Yang S (2012) Long-pulsed 1,064-nm high-energy dye laser improves resistant port wine stains: 20 report cases. *Laser Med Sci* 27(27):1225–1227
6. Yang MU, Yaroslavsky AN, Farinelli WA et al (2005) Long-pulsed neodymium: yttrium-aluminum-garnet laser treatment for port wine stains. *J Am Acad Dermatol* 52:480–490
7. Li D, Farshidi D, Wang GX et al (2014) A comparison of microvascular responses to visible and near-infrared lasers. *Laser Surg Med* 46(6):479–487
8. Jia W, Nadia Tran BS, Victor Sun BS et al (2012) Photocoagulation of dermal blood vessels with multiple laser pulses in an in vivo microvascular model. *Lasers Med Sci* 44(2):144–151
9. Fournier N, Brisot D, Mordon S (2002) Treatment of leg telangiectases with a 532 nm KTP laser in multipulse mode. *Dermatol Surg* 28(7):564–571
10. Wu WJ, Li D, Xing LZ et al (2014) Dynamic characteristics of vascular morphology after 1064 nm laser exposure. *Chin J Lasers* 41(3):0304001-1–0304001-5
11. Aguilar G, Diaz SH, Lavernia EJ et al (2002) Cryogen spray cooling efficiency: improvement of port wine stain laser therapy

- through multiple-intermittent cryogen spurts and laser pulses. *Laser Surg Med* 31(1):27–35
12. Verkruyse W, van Gemert MJ, Smithies DJ et al (2000) Modelling multiple laser pulses for port wine stain treatment. *Phys Med Biol* 45(12):197–203
  13. Hao J, Chen B, Dong L (2017) Dynamic optical absorption characteristics of blood after slow and fast heating. *Laser Med Sci* 32(3): 513–525
  14. Tan OT, Hurwitz RM, Stafford TJ (1996) Single or multiple pulses in the use of the pulsed dye laser for the treatment of port-wine stains. *Laser Med Sci* 11(3):205–210
  15. Tuchin VV, Maksimova IL, Zimnyakov DA et al (1997) Light propagation in tissues with controlled optical properties. *J Biomed Opt* 2(4):401–417
  16. Tuchin VV (2005) Optical clearing of tissues and blood. SPIE Press, Bellingham
  17. Tuchin VV (2005) Optical clearing of tissues and blood using the immersion method. *J Phys D Appl Phys* 38(15):2497–2518
  18. Genina EA, Bashkatov AN, Tuchin VV (2010) Tissue optical immersion clearing. *Expert Rev Med Devic* 7(6):825–842
  19. Zhu D, Larin KV, Luo Q et al (2013) Recent progress in tissue optical clearing. *Laser Photonics Rev* 7(5):732–757
  20. Choi B, Tsu L, Chen E et al (2005) Determination of chemical agent optical clearing potential using in vitro human skin. *Laser Surg Med* 36(2):72–75
  21. Bui AK, McClure RA, Chang J et al (2009) Revisiting optical clearing with dimethyl sulfoxide (DMSO). *Laser Surg Med* 41(2):142–148
  22. Wang RK, Xu X, Tuchin VV et al (2001) Concurrent enhancement of imaging depth and contrast for optical coherence tomography by hyperosmotic agents. *J Opt Soc Am B* 18(7):948–953
  23. Jiang JY, Chen W, Gong QL et al (2010) Study on optical clearing effects by using tissue-like phantom. *Proc SPIE* 7563:75630P-1–75630P-7
  24. Cubeddu R, Pifferi A, Taroni P et al (1997) A solid tissue phantom for photon migration studies. *Phys Med Biol* 42(10):1971–1979
  25. Gracie Vargas MS, Chan EK, Barton JK et al (1999) Use of an agent to reduce scattering in skin. *Laser Surg Med* 24(2):133–141
  26. Vargas G, Barton JK, Welch AJ (2008) Use of hyperosmotic chemical agent to improve the laser treatment of cutaneous vascular lesions. *Biomed Opt* 13(2):21114-1–21114-8
  27. Vargas G, Readinger A, Dozier SS et al (2003) Morphological changes in blood vessels produced by hyperosmotic agents and measured by optical coherence tomography. *Photochem Photobiol* 77(5):541–549
  28. Boergen KP, Birngruber R, Gabel VP, Hillenkamp F (1977) Experimental studies on controlled closure of small vessels by laser irradiation. *Laser Surg Med Biol Proc* 5:15.1–15.9
  29. Stumpp O, Chen B, Welch AJ (2006) Using sandpaper for noninvasive transepidermal optical skin clearing agent delivery. *J Biomed Opt* 11(4):041118-1–041118-9
  30. Xu X, Zhu Q (2007) Evaluation of skin optical clearing enhancement with Azone as a penetration enhancer. *Opt Commun* 279(1): 223–228
  31. Dunn AK, Smithpeter CL, Welch AJ et al (1997) Finite-difference time-domain simulation of light scattering from single cells. *J Biomed Opt* 2(3):262–266
  32. Walter JB, Israel MS (1974) The inflammatory reaction. In: Walter JB (ed) *General pathology*, 4th edn. Churchill Livingstone, London, pp 69–83
  33. Wahl LM, Wahl SM (1992) Inflammation. In: Cohen IK, Diegelmann RF, Lindblad WJ (eds) *Wound healing, biochemical and clinical aspects*. W. B. Saunders Co., Philadelphia, pp 40–53
  34. Langille BL, O'Donnell F (1986) Reductions in arterial diameter produced by chronic decreases in blood flow are endothelium-dependent. *Science* 231(231):405–407
  35. Pfefer TJ, Barton JK, Smithies DJ, Milner TE, Nelson JS, van Gemert MJ, Welch AJ (1999) Modeling laser treatment of port wine stains with a computer-reconstructed biopsy. *Lasers Surg Med* 24(2):151–166